Journal of Histochemistry & Cytochemistry 2018, Vol. 66(2) 99–120

DOI: 10.1369/0022155417741640
journals.sagepub.com/home/jhc
SAGE

Preservation of Functional Microvascular Bed Is Vital for Long-Term Survival of Cardiac Myocytes Within Large Transmural Post-Myocardial Infarction Scar

Colleen Nofi, Yevgen Bogatyryov, and Eduard I. Dedkov
Department of Biomedical Sciences, College of Osteopathic Medicine, New York Institute of Technology, Old Westbury, New York (CN, YB), and Department of Biomedical Sciences, Cooper Medical School of Rowan University, Camden, New Jersey (EID)

Summary

This study was aimed to understand the mechanism of persistent cardiac myocyte (CM) survival in myocardial infarction (MI) scars. A transmural MI was induced in 12-month-old Sprague–Dawley rats by permanent coronary artery ligation. The hearts were collected 3 days, 1, 2, 4, 8, and 12 weeks after MI and evaluated with histology, immunohistochemistry, and quantitative morphometry. Vasculature patency was assessed in 4-, 8-, and 12-week-old scars by infusion of 15-micron microspheres into the left ventricle before euthanasia. The infarcted/scarred area has a small continually retained population of surviving CMs in subendocardial and subepicardial regions. Surprisingly, whereas the transverse area of subepicardial CMs remained relatively preserved or even enlarged over 12 post-MI weeks, subendocardial CMs underwent progressive atrophy. Nevertheless, the fractional volume of viable CMs remained comparable in mature scars 4, 8, and 12 weeks after MI (3.6 ± 0.4%, 3.4 ± 0.5%, and 2.5 ± 0.3%, respectively). Despite the opposite dynamics of changes in size, CMs of both regions displayed sarcomeres and gap junctions. Most importantly, surviving CMs were always accompanied by patent microvessels linked to a venous network composed of Thebesian veins, intramural sinusoids, and subepicardial veins. Our findings reveal that long-term survival of CMs in transmural post-MI scars is sustained by a local microcirculatory bed. (J Histochem Cytochem 66:99–120, 2018)

Keywords

cardiac myocyte survival, microvascular beds, middle-aged rats, myocardial infarction, scar formation, subepicardial veins, Thebesian vessels, venous sinusoids

Introduction

A sudden occlusion of the left coronary artery leads to an acute myocardial infarction (MI) of the left ventricle followed by an inflammatory reaction in the ischemic region and replacement of the necrotic muscle tissue with a fibrous scar.[1,2] As a consequence of thinning and distension of the infarcted region, the left ventricular (LV) cavity dilates causing systolic dysfunction that, in turn, triggers global and regional LV remodeling.[3,4] Although the progressive changes in LV chamber geometry and intrinsic myocardial tissue properties play initially a compensatory role, with time, such alterations become maladaptive and eventually lead to systolic heart failure.[5] Therefore, prevention of MI-induced ventricular wall thinning with various scar-modifying approaches has become one of the fundamental therapeutic strategies that have been extensively explored over the last two decades.[6–9] It is important to emphasize that despite substantial

Received for publication May 22, 2017; accepted October 16, 2017.

Corresponding Author:
Eduard I. Dedkov, Department of Biomedical Sciences, Cooper Medical School of Rowan University, 401 South Broadway, Camden, NJ 08103, USA.
E-mail: dedkov@rowan.edu

Journal of Histochemistry & Cytochemistry

differences among the methodological approaches and therapeutic targets, an ultimate goal for the majority of such strategies is the restoration of the functional myocardium in place of the inert scar tissue.

Traditionally, rats have been routinely utilized in an animal model of experimental MI to study myocardial healing and scar formation.[10–16] More recently, they have become a major subject in evaluating various regenerative, scar-reducing therapies.[17,18] There are two unique features that make rats highly suitable for such purpose. First, rats have an ability to survive after a large MI for an extended period of time permitting the dynamic observation of functional and structural alterations that take place within the damaged area during the post-MI period.[13,16,18] Second, because in the rat heart, the right and left coronary arteries lack intercoronary anastomoses, the permanent ligation in a proximal segment of the left coronary artery always produces a well-demarcated, large, transmural MI.[12,19–21] The latter feature has been proven to be advantageous in detailing a step-by-step chain of cellular and humoral events that underlies the normal healing process in the infarcted myocardium.[10,15] Most importantly, the use of a large and reproducible MI in a rat coronary artery ligation model has been extremely valuable in recognizing the principal methodological challenges encountered by most if not all cell-based regenerative approaches aiming to rebuild the functional myocardium within the ischemic ventricular wall.[17,18]

Considering the persistent failure of various regenerative strategies to quickly and sustainably revascularize a large, chronically ischemic region as well as to either produce the mature cardiac myocytes de novo or continuously retain the transplanted pro-myogenic cells, it is surprising that little attention has been devoted to a comprehensive study of the spared remnants of the viable myocardium, particularly those seen in a central segment of the transmural scars from post-MI rats.[14,15,22–24] Although the regions with viable cardiac myocytes have also been documented within post-MI scars from other animal species, such as mice,[25] cats,[26] dogs,[27–29] rabbits,[26] sheep,[30] as well as humans,[31,32] in the majority of cases, the survival of cardiac myocytes in such areas has been primarily attributed either to continuing arterial blood supply from the non-infarcted myocardium[33] or to a rapid reestablishment of coronary blood flow through the original artery after a brief period of ischemia.[28,30] However, the mechanism of cardiac myocyte survival in a rat model of chronically ischemic LV myocardium remains poorly understood. Moreover, there has been no attempt made to comprehensively investigate a phenotype of such cardiac myocytes and, more important, the microenvironment in which they have resided at different time points after MI.

Therefore, this study was undertaken to characterize the progressive changes in cardiac myocytes that were able to survive in the LV free wall for an extended period of time after permanent ligation of the left coronary artery. Furthermore, a special emphasis has been made on investigation of the regional microenvironment, particularly, the source of nourishing blood supply that would facilitate long-term survival of adult cardiac myocytes in large, fibrous transmural post-MI scars.

Materials and Methods

All experimental procedures were performed in accordance with the *Guide for the Care and Use of Laboratory Animals* published by the National Institutes of Health (NIH Publications No. 85-23, revised 1996).

Animals and Experimental Protocol

A large transmural MI was induced in 12-month-old male (*n*=52) Sprague–Dawley rats (Charles River Laboratories, Inc.; Wilmington, MA) under ketamine (100 mg/kg intraperitoneal [i.p.]) and xylazine (10 mg/kg i.p.) anesthesia by permanent ligation of the left anterior descending coronary artery near its origin, as previously detailed elsewhere.[12,15] Sham-operated rats (*n*=6) served as age-matched controls. Following surgery, the rats were housed under climate-controlled conditions at a 12-hr light/dark cycle, and provided with standard rat chow and water ad libitum. The mortality rate among post-MI rats was ~30% with all death occurring within the first 48 hr. The survived rats were euthanized 3 days, 1, 2, 4, 8, and 12 weeks after MI (*n*=6 per experimental group), and their hearts were collected for further evaluation.

In three groups of post-MI rats (4, 8, and 12 weeks after surgery) in which the formation of scar tissue has been completed,[15] shortly before collecting the hearts, non-radioactive microspheres, 15 μm in diameter, were delivered into the LV chamber of beating hearts to assess the potency of blood vessels in the scars. Briefly, each rat was anesthetized with 3% isoflurane in pure oxygen, and a polyethylene catheter (PE-50), attached to a fluid-filled, blood pressure transducer, was inserted into the right common carotid artery and advanced into the left ventricle under the guidance of a pressure waveform. Approximately 1 million microspheres in 0.4 ml of saline (BioPAL, Inc.; Worcester, MA) were infused over 5 sec into the LV chamber with a syringe.

Table 1. Primary Antibodies Used for Immunostaining.

Antigen	Host	Clone	Isotype	Dilution	Catalog No.	Source
Actin, cardiac	Mouse	AC1-20.4.2	IgG1	1:100	A9357	Sigma; St. Louis, MO
Alpha-Smooth Muscle Actin	Mouse	1A4	IgG2a	1:600	A2547	Sigma; St. Louis, MO
Connexin 43	Mouse	—	IgG1	1:300	MAb3068	Millipore; Temecula, CA
Desmin	Mouse	DE-U-10	IgG1	1:80	D1033	Sigma; St. Louis, MO
Laminin	Rabbit	—	—	1:60	L9393	Sigma; St. Louis, MO
Myosin, cardiac (β-isoform)	Mouse	NOQ7.5.4D	IgG1	1:1000	M8421	Sigma; St. Louis, MO

At the end of each time period, rats under isoflurane anesthesia were weighed, and the hearts were arrested in diastole by an intracardiac injection of potassium chloride, excised from the thorax, attached to a Langendorff apparatus and were perfusion-fixed with 4% paraformaldehyde (PFA) in phosphate-buffered saline (PBS) for 20 min at constant pressure (100 mmHg). Then, the hearts were immersed in a fresh portion of 4% PFA solution and stored at +4C for 48 hr, before being processed for infarct size measurements and tissue sampling.

Post-MI rats were included in the final evaluation only if the size of the transmural infarct zone/scar was equal or greater than 50% of the LV free wall. Furthermore, the quantitative assessment of the LV chamber remodeling, scar thinning, and the fractional volume of the cardiac myocytes surviving within the scars were only conducted 4, 8, and 12 weeks after MI, because at these time periods the transmural scars had a relatively similar level of maturation.

Determination of Infarct Size and Tissue Sampling

In each heart, the atria and the right ventricular free wall were removed, and the left ventricle, including septum, was cut transversely from apex to the base into five parallel slices with a blade guillotine. Then, the LV slices were briefly blotted dry with filter paper and weighed.

To determine the infarct/scar size, all LV slices from the heart were digitized into a computer using a Motic K-400L stereo microscope (Motic Instruments, Inc.; Richmond, BC, Canada) equipped with an Olympus DP70 digital camera (Olympus America, Inc.; Center Valley, PA) and then measured with Image-Pro Analyzer 7.0 software (Media Cybernetics, L.P.; Silver Spring, MD), as detailed previously.[13] Briefly, in each digitized slice, the lengths of the entire free wall and its infarcted/scarred portion (both obtained at the mid-wall level) were determined. The extent of the transmural infarcted/scarred area in each LV slice was estimated as the ratio between the length of the infarcted zone/scar and the length of the total free wall, and then the mean of these ratios was calculated. Finally, the infarct size was expressed as a percentage of the LV free wall.

From each heart, the two midventricular LV slices were processed into paraffin blocks for histological analysis.

Histology and Immunohistochemistry

Transverse, 8.0-μm-thick serial sections were cut from the paraffin-embedded LV slices onto microscope slides. From each LV slice, several sections were routinely stained with Masson's trichrome and hematoxylin and eosin (H&E) stains.

Other serial sections were subjected to immunolabeling with various combinations of the primary (Table 1) and secondary (Table 2) antibodies or stained with Griffonia Simplicifolia isolectin IB_4 (GS-IB_4). Briefly, sections were deparaffinized and antigen retrieval was performed by enzyme digestion either with 0.025% trypsin (cat. T4424; Sigma, St. Louis, MO) or with 20 mg/ml proteinase K (cat. P4850; Sigma, St. Louis, MO) in Dulbecco's PBS containing calcium and magnesium ions (cat. 14040; Life Technologies, Carlsbad, CA) for 20 min at 37C. Incubation with primary antibodies was conducted for 2.0 hr followed by labeling with fluorophore-conjugated secondary antibodies or GS-IB_4 lectin for 45 min at 37C in a moist chamber. The sections were coverslipped with ProLong Gold antifade mounting medium (cat. P36931; Molecular Probes, Inc., Eugene, OR) containing DAPI (4′,6-diamidino-2-phenylindole) to counterstain the nuclei. Omission of primary antibodies or GS-IB_4 lectin served as negative controls.

Microscopy and Quantitative Morphometry

The entire profiles of the LV cross-sections stained with Masson's trichrome and H&E were captured onto

Table 2. Fluorophore-Conjugated Secondary Antibodies and Lectins Used for Fluorescence Staining.

Description	Dilution	Catalog No.	Source
Alexa Fluor 488-conjugated goat anti-mouse IgG (H + L)	1:200	A-11001	Molecular Probes; Eugene, OR
Alexa Fluor 594-conjugated goat anti-mouse IgG (H + L)	1:400	A-11032	Molecular Probes; Eugene, OR
Alexa Fluor 488-conjugated goat anti-rabbit IgG (H + L)	1:200	A-11008	Molecular Probes; Eugene, OR
Alexa Fluor 594-conjugated isolectin GS-IB_4	10 µg/ml	I21413	Molecular Probes; Eugene, OR
Alexa Fluor 488-conjugated isolectin GS-IB_4	20 µg/ml	I21411	Molecular Probes; Eugene, OR
Rhodamine Red-X-conjugated goat anti-mouse IgG (H + L)	1:200	115-295-146	Jackson ImmunoResearch Lab.; West Grove, PA
Cy3-conjugated goat anti-mouse IgG ($F_{C\gamma}$ subclass 2a)	1:400	115-165-206	Jackson ImmunoResearch Lab.; West Grove, PA
Cy3-conjugated goat anti-mouse IgG (H + L)	1:400	115-165-166	Jackson ImmunoResearch Lab.; West Grove, PA

Abbreviation: GS-IB_4, Griffonia Simplicifolia isolectin IB_4.

a computer using a Motic K-400L stereo microscope (Motic Instruments, Inc.) equipped with an Olympus DP70 digital camera (Olympus America, Inc.) and then measured with Image-Pro Analyzer 7.0 software (Media Cybernetics, L.P.), as detailed previously.[13] The following planimetric parameters of the left ventricle were acquired using these images: the cross-sectional areas (CSAs) of the left ventricle and its cavity, and the average thicknesses of the septum and the scar. From these measurements, the scar thinning ratio and expansion index (a parameter that reflects the degree of LV dilatation and scar thinning) were determined as follows: The scar thinning ratio was calculated as the ratio between average thickness of the scar and the average thickness of the septum, whereas the expansion index was calculated as (LV cavity area/LV area) × (septal wall thickness/scar thickness).

The LV cross-sections stained with Masson's trichrome were examined under the Olympus BX53 microscope (Olympus America Inc.) and, in each section, the series of high-resolution images covering the entire scar region were captured with an Olympus DP72 digital camera. Digital assembly of the complete scar profiles from the captured images was done using Adobe Photoshop CC software (Adobe Systems; San Jose, CA). Using a reconstructed, high-resolution image of each individual scar, the total profile of the scar was thoroughly outlined, and its area was measured with Image-Pro Analyzer 7.0 software. Finally, a color image segmentation technique was applied to each scar to determine the fractional volume of the surviving cardiac myocytes within the scar, as described previously.[14] Briefly, a digital color image of the scar stained with Masson's trichrome was partitioned by using Image-Pro Analyzer 7.0 software into discrete segments based on color similarity between the areas occupied with viable muscle cells. Utilizing this approach, the total area of surviving cardiac myocytes was determined in each scar, and then the fractional volume of surviving cardiac myocytes was expressed as a percentage of the total scar volume.

The double and triple fluorescence labeled sections were examined under the Olympus BX53 fluorescence microscope, and individual images were captured onto a computer with an Olympus DP72 digital camera. Finally, separate, single-color images of the same fields were combined using Olympus cellSens Standard 1.4.1 digital imaging software (Olympus America Inc.) to produce the multicolored composites.

The merged digital images from the sections co-stained with the antibodies against β-cardiac myosin and laminin, and counterstained with DAPI, were used to determine the mean CSA of cardiac myocytes surviving in subendocardial and subepicardial regions of the transmural scars. To avoid the analysis of cardiac myocytes that could be still connected to viable myocardium at the edges of the scar, only areas of the transmural scars remote from the remaining myocardium by at least 1.5–2 mm were used in this assessment. Briefly, the laminin-outlined profiles of β-cardiac myosin-positive myocytes were electronically traced by using an Image-Pro Analyzer 7.0 software (Media Cybernetics, L.P.), and their diameters, aspect ratios, and CSAs were measured. In average, about 60–100 cardiac myocyte profiles per subendocardial and subepicardial regions were analyzed in each scar. Finally, to estimate the mean CSA of surviving myocytes, only cells with an aspect ratio of less than 2.5 times and containing a round-shaped nucleus were used.

At the same time, the merged digital images from the sections co-stained with a GS-IB4 lectin and an antibody against α-smooth muscle (SM) actin, and counterstained with DAPI, were utilized to determine the diameter of blood vessels accompanying the surviving cardiac myocytes in subendocardial and subepicardial regions of the transmural scars. Briefly, the

lumen of lectin- and/or α-SM actin-outlined vascular profiles were electronically traced by using an Image-Pro Analyzer 7.0 software (Media Cybernetics, L.P.), and their diameters were calculated.

Statistical Analysis

Data are expressed as the Mean ± SD. Statistical analysis was performed using Prism 6 software package (IBM Corp.; Armonk, NY). A one-way analysis of variance (ANOVA) followed by the Tukey's post hoc tests were performed for multigroup comparisons. A one-tailed unpaired Student's *t*-test was used to assess the difference between two groups. A probability of $p \leq 0.05$, $p \leq 0.01$, and $p \leq 0.001$ were considered to indicate different levels of statistical significance.

Results

Considering the highly dynamic nature of structural changes within the infarcted region, several sequential time points, including 3 days, 1, 2, 4, 8, and 12 weeks post-MI, were used to evaluate cardiac myocyte survival in progression, during scar formation, and remodeling. Because at the edges of the scar the surviving cardiac myocytes could still receive uninterrupted arterial blood supply from the vessels originating in adjacent non-infarcted regions, the principal focus was on cells remaining in a central zone of the scars, which were evidently remote from the scar edges and, thereby, had no access to a conventional route of arterial blood supply. Furthermore, to determine whether scar maturation could affect the long-term viability of the remaining cells, the fractional volume of surviving cardiac myocytes as well as the functional potency of the blood vessels associated with them have been assessed in mature 4-, 8-, and 12-week-old post-MI scars.

Cardiac Myocytes Are Capable of Long-Term Survival in Large Transmural Post-MI Scars

The evaluation of post-MI hearts throughout 12 weeks following permanent ligation of the left coronary artery revealed that large transmural scars of the left ventricle contained a sparse population of viable cardiac myocytes (Figs. 1, 2, and 3). At all time periods, a majority of surviving cardiac myocytes was noticed as thin discontinuous layers in 2 distinct regions of each scar, one beneath the endocardium and another beneath the epicardium (Figs. 1A, B; 2A, C, and 3A). Furthermore, in the subepicardial region, large clusters of viable cardiac myocytes were often associated with large subepicardial veins with a mean diameter of 98.2 ± 19.5 µm (Figs. 1D, 2B, D, and 3B), whereas, in subendocardial regions, the isolated groups of surviving cardiac myocyte were occasionally seen around the venous channels resembling Thebesian vessels (Fig. 1C). Moreover, during the first few weeks of scar formation, the viable cardiac myocytes were periodically detected deep in intramural regions where they surrounded thin-walled sinusoidal vessels with a mean diameter of 25.5 ± 4.2 µm (Fig. 2A: asterisks).

Most importantly, the quantitative assessment of mature scars demonstrated that the fractional volume of surviving cardiac myocytes remained relatively comparable between the fourth and twelfth post-MI weeks in hearts that had similar-sized infarcts and the analogous scale of LV chamber remodeling (Table 3).

Cardiac Myocytes Remaining in Subepicardium and Subendocardium of Post-MI Scars Demonstrate the Region-Dependent Dynamics of Changes in Size

Despite the fact that viable cardiac myocytes were concurrently present in two specific areas of each transmural scar, that is, subendocardial and subepicardial regions, the quantitative assessment of their transverse profiles revealed that the cells in these two areas have undergone markedly different alterations in size during the course of 12 post-MI weeks. While the cardiac myocytes residing in subepicardium preserved and, to some degree, even increased their CSAs, compared with the cells from the similar areas in control hearts, the cardiac myocytes remaining in subendocardium exhibited noticeable atrophy (Fig. 4).

Viable Cardiac Myocytes of Post-MI Scars Persistently Maintain Sarcomeric Organization and Expression of Gap Junction Protein Connexin 43

The examination of longitudinal and oblique profiles of the cardiac myocytes surviving in subepicardial and subendocardial regions of the post-MI scars has revealed that a substantial number of remaining cells were able to preserve the characteristic arrangement of contractile and supporting proteins into organized sarcomeres (Fig. 5). Moreover, the noticeable atrophy seen in subendocardial myocytes did not prohibit the long-term maintenance of sarcomeric organization of the contractile apparatus in such cells (Fig. 5C and D).

In addition, the immunodetection of gap junction protein connexin 43 in viable cardiac myocytes remaining in subendocardial and subepicardial regions of post-MI scars demonstrated that connexin 43 proteins were

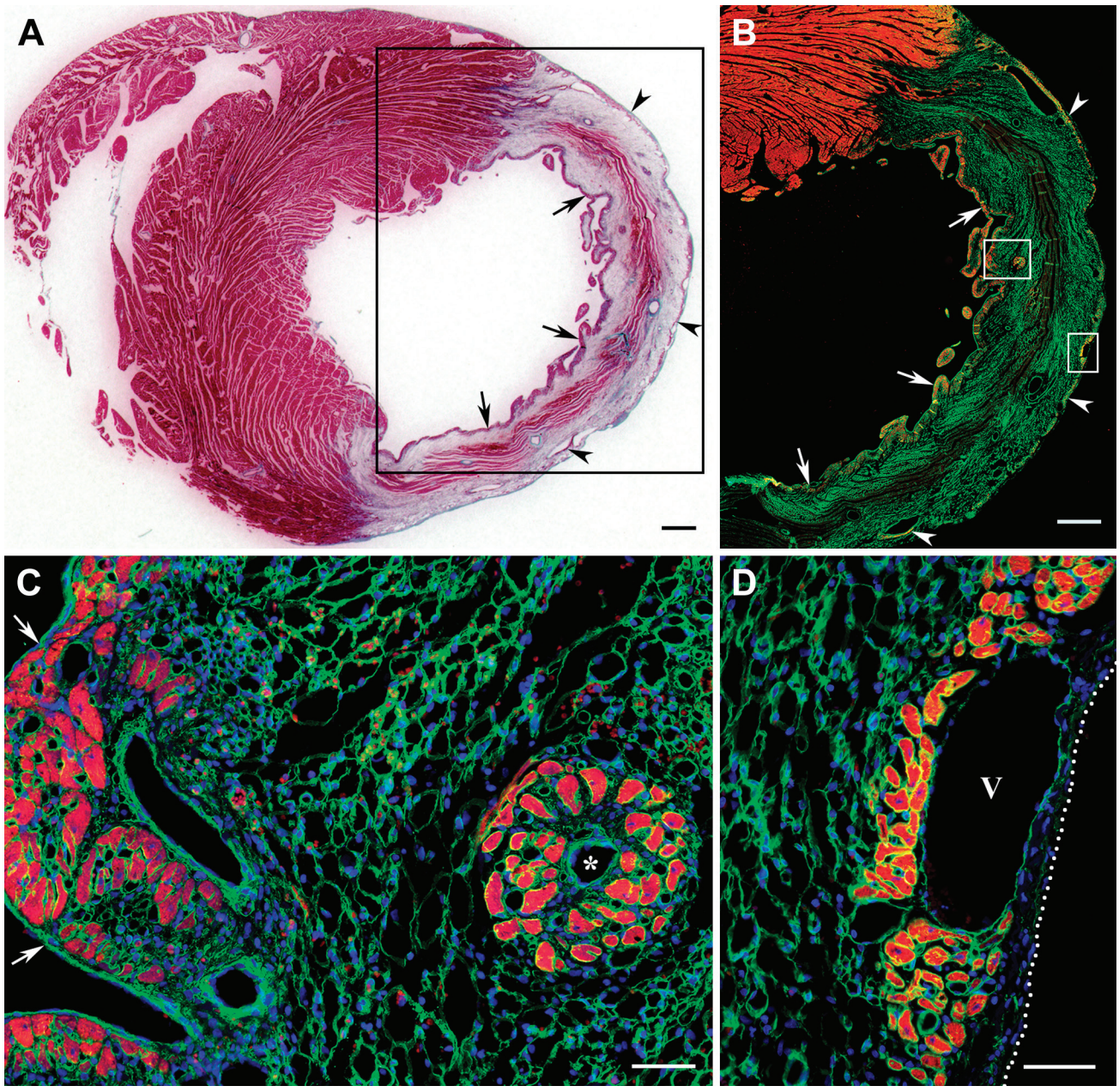

Figure 1. Distribution of surviving cardiac myocytes in a representative 1-week-old transmural post-MI scar visualized with Masson's trichrome stain (dark red color in A) and double immunofluorescence staining (B–D) with antibodies against cardiac MHC β-isoform (red color) and laminin (green color). In C and D, nuclei are counterstained with DAPI (blue color). (A) Transverse section through the midventricular level of the post-MI heart demonstrating the presence of viable cardiac myocytes in subendocardial (arrows) and subepicardial (arrowheads) regions of the scar. Note that muscle-specific staining (dark red color) seen within the middle region of the scar is associated entirely with the remnants of dead mummified myocytes. (B) Immunofluorescence micrograph of the area outlined by a black box in A showing the viable cardiac myocytes in subendocardial (arrows) and subepicardial (arrowheads) regions of the same scar obtained on an adjacent serial section. Note that remnants of dead mummified myocytes located in the middle region of the scar remain unstained with antibody against cardiac MHC β-isoform (red color), although most of them continue to be outlined by laminin-positive basement membranes. (C) High-power view of the subendocardial region outlined by a white box in B demonstrating the arrangement of viable cardiac myocytes in the discontinuous layer just beneath the endocardium (arrows) as well as in the isolated cluster around a small, thin-walled venous-like vascular channel, which resembles a Thebesian vein or vessel (asterisk). (D) High-power view of the subepicardial region outlined by a white box in B showing the groups of viable cardiac myocytes beneath the epicardium (white dotted line) in close proximity to a large subepicardial vein (V). Scale bars are 600 μm (A, B) and 50 μm (C, D). Abbreviations: MI, myocardial infarction; MHC, myosin heavy chain; DAPI, 4′,6-diamidino-2-phenylindole.

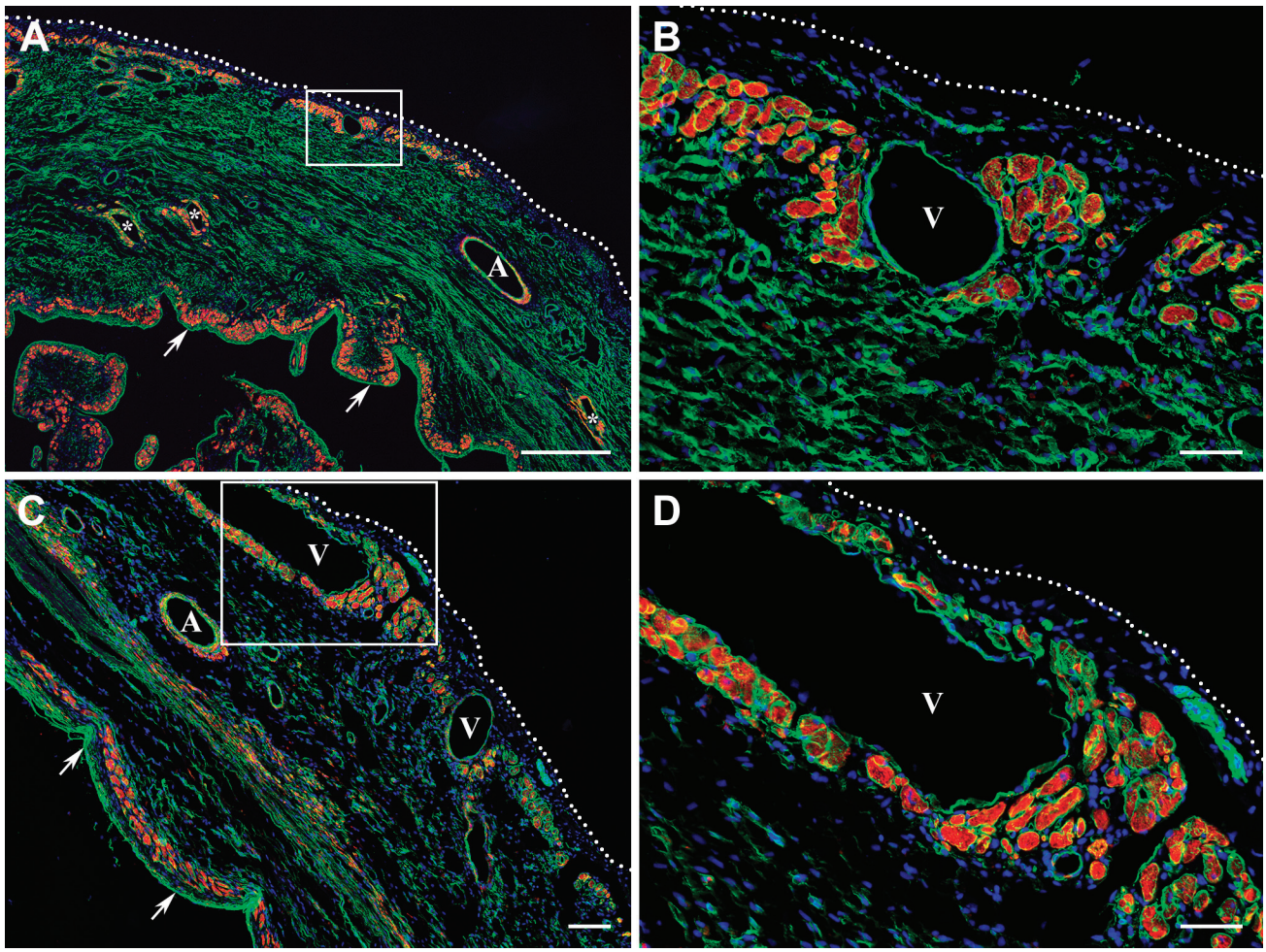

Figure 2. Distribution of surviving cardiac myocytes in the representative 2-week-old (A, B) and 4-week-old (C, D) transmural post-MI scars visualized by double immunofluorescence staining with antibodies against desmin (red color) and laminin (green color). In all micrographs, nuclei are counterstained with DAPI (blue color). (A and C) Low-power views of the transmural scars demonstrating the discontinuous layers of viable cardiac myocytes beneath the endocardium (arrows) and epicardium (white dotted line). In A, a few isolated clusters of surviving cardiac myocytes are seen intramurally, surrounding the thin-walled sinusoidal vessels (asterisks). It is important to note that in comparison with subepicardial veins (V), the walls of large coronary arteries (A) are composed of desmin-positive vascular smooth muscle cells. Furthermore, a patchy pattern of red immunofluorescence staining detected in the middle portion of the scar extending along the compact laminin-positive bundles presumably belongs to the desmin-expressing myofibroblasts. (B and D) High-power views of the subepicardial regions outlined by the corresponding white boxes in A and C, respectively, demonstrating the large groups of surviving cardiac myocytes just beneath the epicardium (white dotted line) and near the large subepicardial veins (V). Scale bars are 500 μm (A), 100 μm (C), and 50 μm (B, D). Abbreviations: MI, myocardial infarction; DAPI, 4′,6-diamidino-2-phenylindole; MHC, myosin heavy chain.

consistently distributed on the interfacing surfaces between adjacent myocytes in the pattern seemingly resembling typical gap junctions (Fig. 6: arrowheads).

Cardiac Myocytes Surviving in Post-MI Scars Are Supported by Functional Microvascular Networks

The progressive evaluation of two discontinuous layers of surviving cardiac myocytes located in subendocardial and subepicardial regions of the transmural scars has revealed that at all time periods examined, the viable cardiac myocytes were surrounded by the networks of functional microvessels, which were predominantly composed of capillaries and postcapillary venules (Fig. 7). Moreover, in both regions, the well-organized microvascular beds were always seen within clusters of surviving myocytes surrounding large veins. More importantly, the microvascular network supporting the viable cardiac myocytes throughout 12 post-MI weeks remained relatively unaffected by the process of scar maturation during which a majority of newly

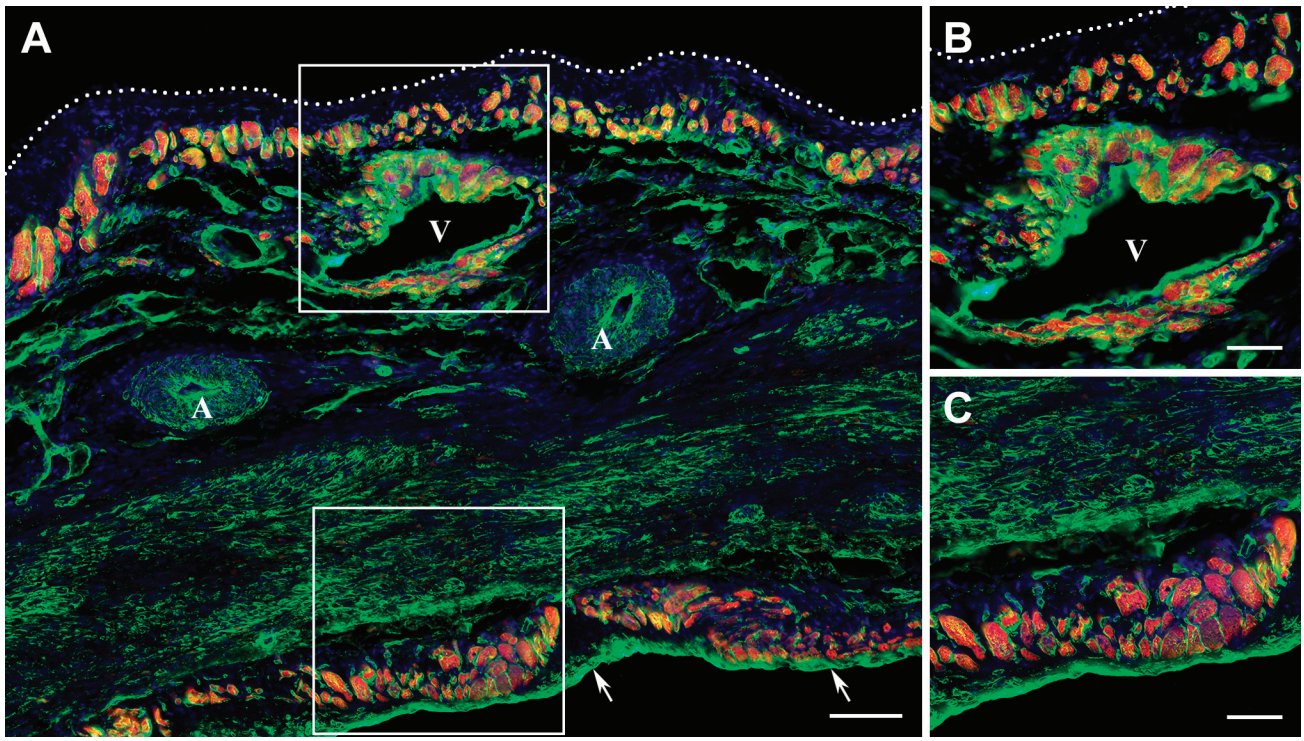

Figure 3. Distribution of surviving cardiac myocytes in a representative 12-week-old transmural post-MI scar visualized by double immunofluorescence staining with antibodies against cardiac MHC β-isoform (red color) and laminin (green color). In all micrographs, nuclei are counterstained with DAPI (blue color). (A) Low-power view of the scar demonstrating the discontinuous layers of viable cardiac myocytes beneath the endocardium (arrows) and epicardium (white dotted line). Note that viable cardiac myocytes are present around a large vein (V), whereas they are completely absent in the vicinity of coronary arteries (A). (B) High-power view of the subepicardial region outlined by the white box in A showing the viable cardiac myocytes beneath the epicardium (white dotted line) and around the large subepicardial vein (V). (C) High-power view of the subendocardial region outlined by a white box in A demonstrating the viable cardiac myocytes beneath the endocardium. Scale bars are 100 μm (A) and 50 μm (B, C). Abbreviations: MI, myocardial infarction; MHC, myosin heavy chain; DAPI, 4′,6-diamidino-2-phenylindole.

Table 3. Left Ventricular Structural Parameters and Fractional Volume of Surviving Cardiac Myocytes in the Transmural Myocardial Infarction Scars.

	4wkMI	8wkMI	12wkMI
n	6	6	5
Infarct size (% of LVFW)	64.9 ± 11.8	63.3 ± 10.1	61.6 ± 6.4
LV weight/BW ratio (mg/g)	2.23 ± 0.29	2.38 ± 0.21	2.51 ± 0.31
LV CSA (mm^2)	100.5 ± 16.8	108.9 ± 11.6	114.9 ± 15.8
LV cavity CSA (mm^2)	48.9 ± 9.8	50.5 ± 4.5	55.3 ± 14.4
Septal wall thickness (mm)	1.80 ± 0.32	1.98 ± 0.34	2.14 ± 0.56
Scar thickness (mm)	0.88 ± 0.16	0.93 ± 0.30	0.92 ± 0.22
Scar thinning ratio	0.49 ± 0.09	0.48 ± 0.16	0.47 ± 0.17
Expansion index	1.02 ± 0.25	1.07 ± 0.36	1.12 ± 0.34
Scar CSA, mm^2	12.9 ± 2.7	11.6 ± 2.9	14.5 ± 2.4
Surviving CM per scar, %	3.6 ± 1.2 (1.7–5.7)	3.4 ± 1.3 (1.8–5.1)	2.5 ± 0.9 (1.2–4.1)

Values are Mean ± SD; Scar thinning ratio = scar thickness/septal wall thickness; Expansion index = (LV cavity CSA/LV CSA) × (septal wall thickness/scar thickness). Abbreviations: *n*, number of rats; MI, myocardial infarction; LVFW, left ventricular free wall; LV, left ventricular; BW, body weight; CSA, cross-sectional area; CM, cardiac myocytes.

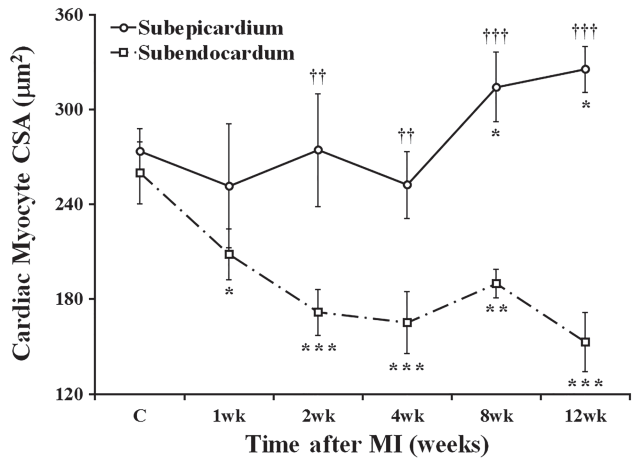

Figure 4. Time course of changes in CSA of the cardiac myocytes surviving in subepicardial and subendocardial regions of the transmural scar during 12 post-MI weeks. Data are Mean ± SD; *$p<0.05$, **$p<0.01$, and ***$p<0.001$ versus cardiac myocytes in corresponding groups of the control rats (C); $^{\dagger\dagger}p<0.01$ and $^{\dagger\dagger\dagger}p<0.001$ versus cardiac myocytes in subendocardial region of the same rats. Abbreviations: CSA, cross-sectional area; MI, myocardial infarction.

formed capillaries disappeared from the granulation tissue when it had transformed in an avascular fibrous scar tissue (Fig. 7C–H).

At the same time, immunostaining against α-SM actin has shown that although small arteriolar-type resistance vessels became almost undetectable among surviving cardiac myocytes in 3-day-old MI (data not shown), they have clearly reappeared in the transmural scars beginning with week 1 following permanent coronary artery ligation and then remained identifiable for the duration of 12 post-MI weeks (Fig. 8). However, based on the phenotypic appearance of these newly developed resistance-like microvessels, it seemed that the vast majority of such vessels did not belong to typical arteriolar vessels (Fig. 8A: double arrow), but rather resembled arterialized thin-walled venous vessels, such as postcapillary venules with a mean diameter of 15.2 ± 4.2 μm (Fig. 8: arrowheads) and small veins (Fig. 8: asterisks).

Blood Vessels Supplying Viable Cardiac Myocytes in Post-MI Scar Are Coupled With the Venous System Composed of Thebesian Veins, Venous Sinusoids, and Subepicardial Veins

The further assessment of macrovascular structures seen in close proximity with the surviving cardiac myocytes in the transmural scars revealed that they belong to the various elements of the preexisting venous system of the LV wall that were spared during MI. The most obvious elements of such system were intramural venous sinusoids (Figs. 9A, C, and 10A, B) and large subepicardial veins (Fig. 9B), whereas the orifices linking the Thebesian veins or venous channels with LV cavity were relatively rare (Fig. 10: arrows). The close association between either subendocardial microvessels or thin-walled sinusoids, which were surrounded by viable cardiac myocytes, and Thebesian veins originating from the LV lumen (Fig. 10: arrowheads), suggest probable functional coupling between these vascular structures.

Vascular Beds Accompanying Viable Cardiac Myocytes in Post-MI Scars Retain Potency for Persistent Blood Flow in the Presence of Permanently Ligated Left Coronary Artery

To verify that in transmural scars, the residual venous system was capable of sustainable blood delivery into the vascular beds supporting viable cardiac myocytes in both subepicardial and subendocardial regions, 15-micron microspheres were infused in LV cavity 4, 8, and 12 weeks following permanent ligation of the left coronary artery. The microspheres were persistently detected in the venular vessels (Fig. 11: arrows) either adjacent to or within the clusters of surviving cardiac myocytes located in subendocardium as well as subepicardium of the transmural scars (Fig. 12: asterisks). This suggests the existence of a patent route for arterial blood circulation from the LV cavity, via Thebesian vessels, toward subepicardial veins.

Discussion

The key findings of this study were as follows: (1) adult (mature) cardiac myocytes residing in subendocardial and subepicardial regions of the LV free wall of middle-aged rats were capable of prolonged survival within a large, transmural post-MI scar caused by permanent ligation of the left coronary artery; (2) the fractional volume of viable cardiac myocytes remained relatively similar in scars between 4 and 12 post-MI weeks, although cells surviving in subendocardium had undergone substantial atrophy compared with those in subepicardial region; (3) the viable cardiac myocytes seen in remote, isolated groups continued to demonstrate a mature phenotype for the duration of 12 post-MI weeks, including the organized array of sarcomeres and connexin 43-positive gap junctions; (4) in all regions of the scar, the groups of surviving cardiac myocytes were always accompanied by a network of patent microvessels; (5) the microcirculatory beds supplying the viable

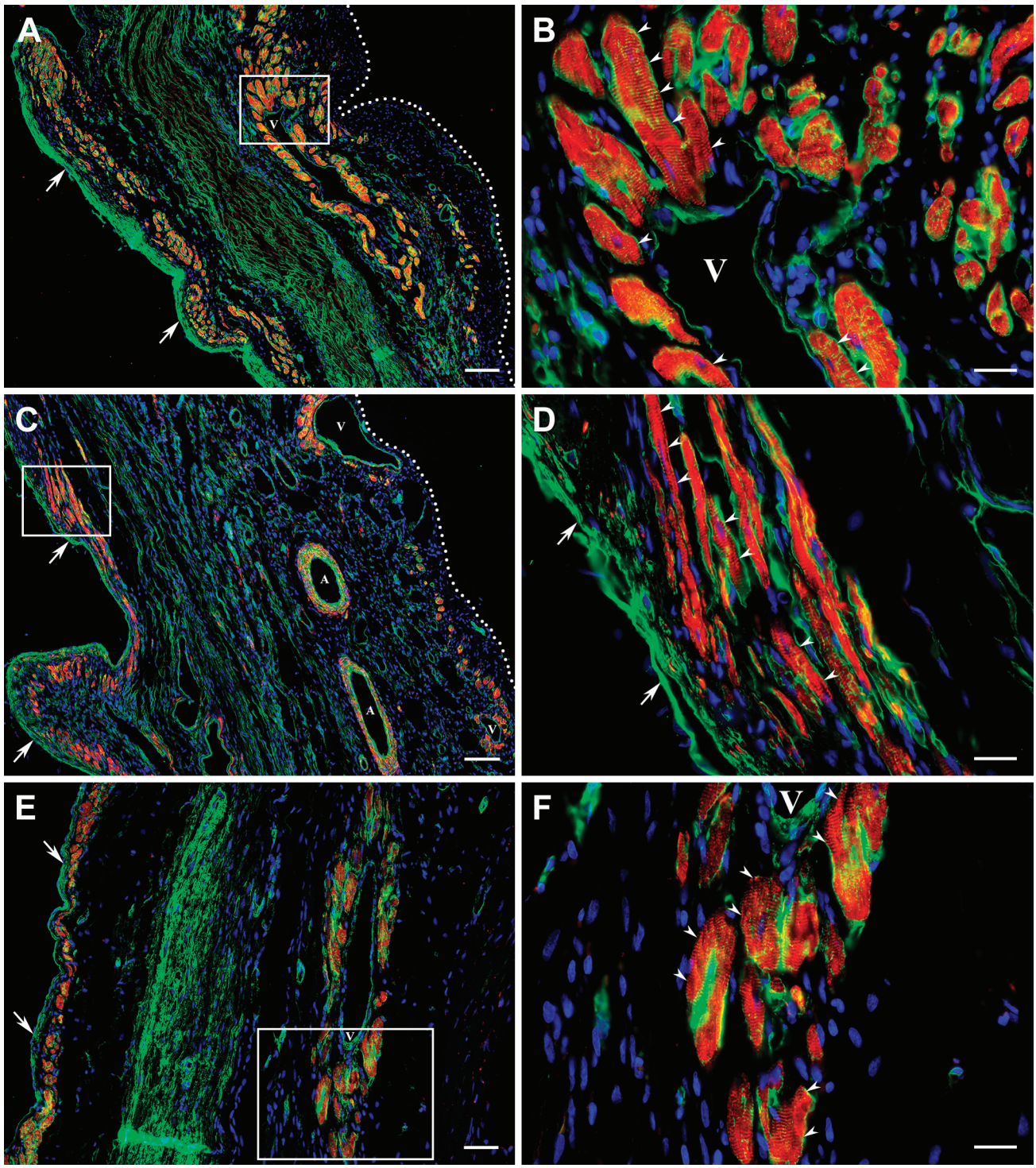

Figure 5. Immunofluorescence micrographs demonstrating the organized sarcomeric striations in cardiac myocytes surviving within 4-week-old (A–D) and 8-week-old (E, F) transmural post-MI scars. The viable cardiac myocytes (red color) are visualized using double immunostaining with antibodies against either cardiac actin (A, B, C, and D) or desmin (C, D) and laminin (green color). In all micrographs, nuclei are counterstained with DAPI (blue color). (A, C, E) Low-power views of the scars demonstrating the discontinuous layers of viable cardiac myocytes beneath the endocardium (arrows) and epicardium (white dotted line in A and C). Note that, in all scars, the clusters of surviving cardiac myocytes are present in close proximity to the large venous vessels (V). It is important to notice that desmin-positive immunostaining in the walls of large coronary arteries (A) is associated with the presence of vascular smooth muscle cells. (B, D, F) High-power views of the regions outlined by the corresponding white boxes in A, C, and E, respectively, exposing the sarcomeric striations in viable cardiac myocytes (arrowheads) surviving beneath the endocardium (arrows in D) and near the large venous vessels (V) located in the subepicardial area. Scale bars are 50 μm. Abbreviations: MI, myocardial infarction; DAPI, 4′,6-diamidino-2-phenylindole.

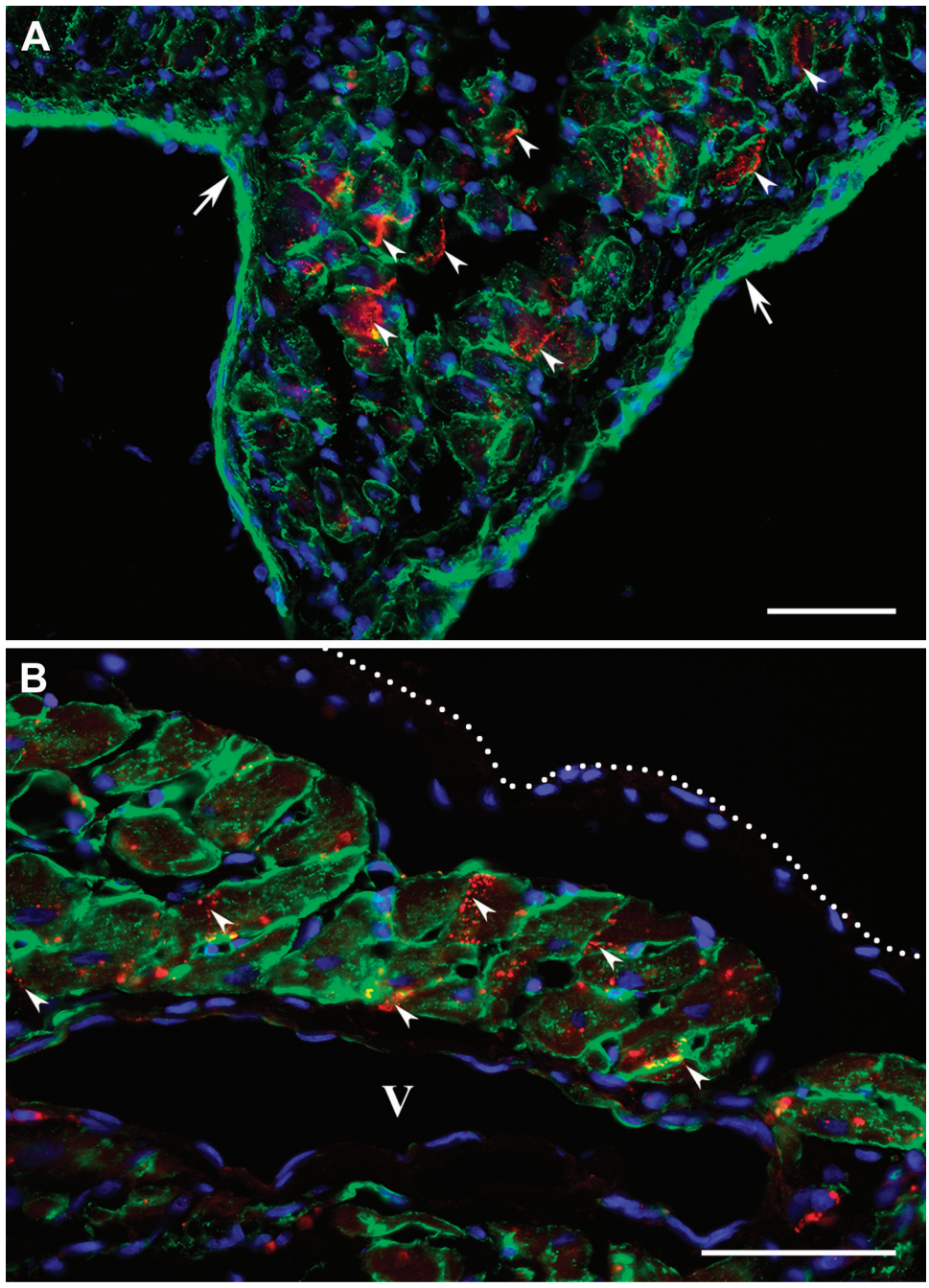

Figure 6. Immunofluorescence micrographs displaying the gap junctions between cardiac myocytes surviving within 2-week-old (A) and 4-week-old (B) transmural post-MI scars. The viable cardiac myocytes are outlined using an antibody against laminin (green color), whereas the locations of gap junctions are visualized with an anti-connexin 43 antibody (red color). In both micrographs, nuclei are counterstained with DAPI (blue color). (A) High-power view showing surviving cardiac myocytes beneath the endocardium (arrows). (B) High-power view demonstrating surviving cardiac myocytes in close proximity to a large venous vessel (V) beneath the epicardium (white dotted line). Note that in A and B, the connexin 43 is accumulated on the lateral sides of viable cardiac myocytes displaying the typical gap junction arrangement along the interfacing surfaces of adjacent myocytes (arrowheads). Scale bars are 50 μm. Abbreviations: MI, myocardial infarction; DAPI, 4′,6-diamidino-2-phenylindole.

cardiac myocytes within the scars were functionally coupled with the residual system of venous vessels composed of Thebesian veins or venous channels, intramural sinusoids, and subepicardial veins.

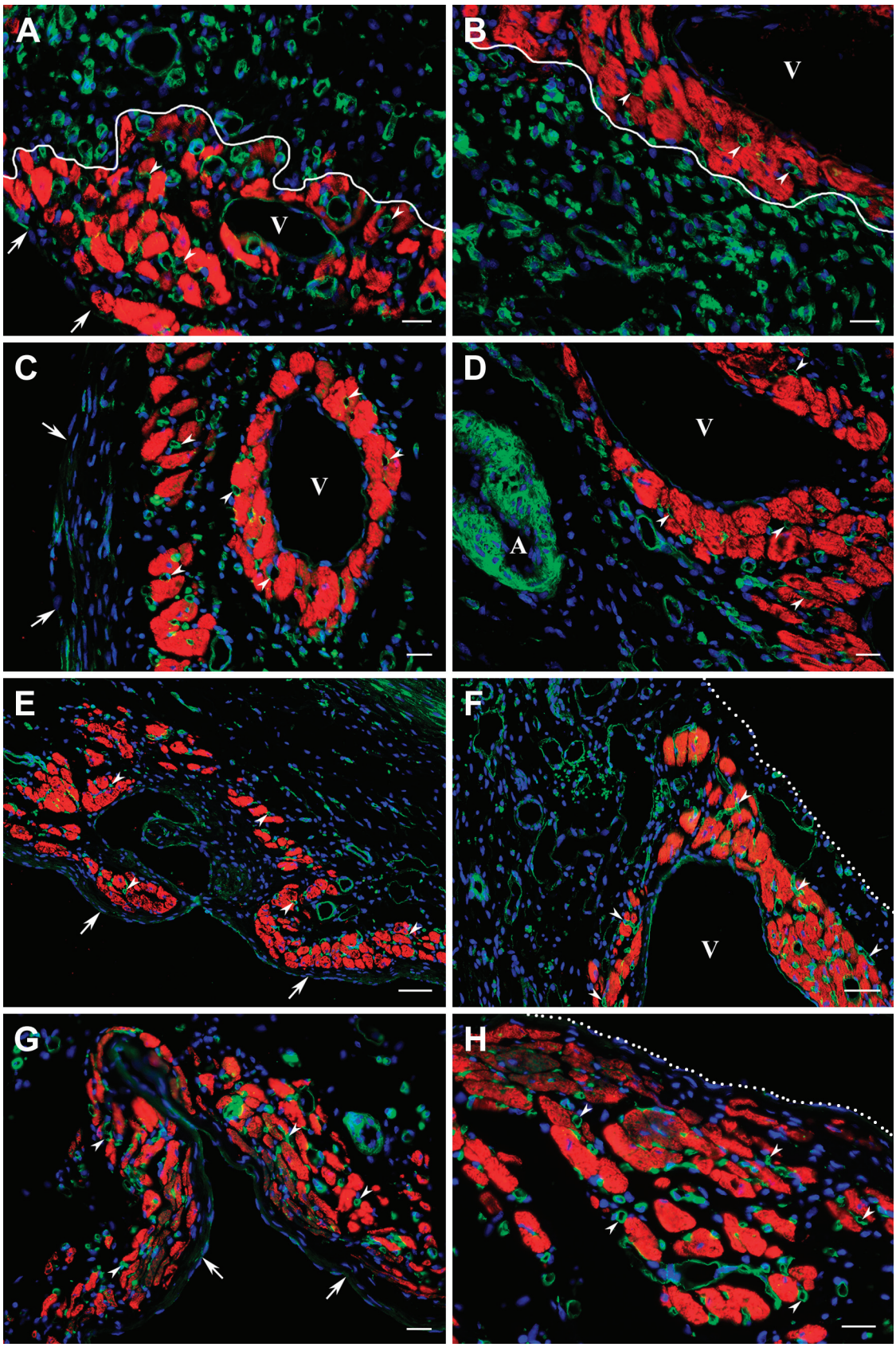

(continued)

Figure 7. Immunofluorescence micrographs demonstrating the presence of functional capillaries among the viable cardiac myocytes in 1-week-old (A, B), 2-week-old (C, D), 8-week-old (E, F), and 12-week-old (G, H) transmural post-MI scars. The cardiac myocytes surviving within subendocardial (A, C, E, G) and subepicardial (B, D, F, H) regions of the corresponding scars are visualized using immunostaining with an antibody against cardiac MHC β-isoform (red color), whereas capillaries (arrowheads) and other vascular structures, including veins (V) and arteries (A), are revealed with the GS-IB_4 lectin staining (green color). Note that in the wall of a former coronary artery, the GS-IB_4 lectin-positive staining is associated with both endothelial and smooth muscle cells. In all micrographs, nuclei are counterstained with DAPI (blue color). In A, C, E, and G, arrows point to the endocardium, whereas in F and H, the white dotted lines mark the epicardial border. Furthermore, in A and B, a white solid line separates the groups of surviving cardiac myocytes from the highly vascularized granulation tissue. It is important to emphasize that all clusters of long-term surviving cardiac myocytes seen beneath the endocardium (A, C, E, G) and epicardium (B, D, F, H), including those surrounding the large veins (A–D and F), expose the presence of well-organized capillary networks. Moreover, the capillary beds accompanying the viable cardiac myocyte for the duration of 12 post-MI weeks remain generally preserved even during maturation of the granulation tissue—a process associated with the disappearance of a majority of microvessels from the scar. Scale bars are 20 μm (A–D, G, and H) and 50 μm (E, F). Abbreviations: MI, myocardial infarction; MHC, myosin heavy chain; GS-IB_4, Griffonia Simplicifolia isolectin IB_4; DAPI, 4′,6-diamidino-2-phenylindole.

Are Long-Term Surviving Cardiac Myocytes in Transmural Post-MI Scar Similar to Those in Chronically Ischemic, "Hibernating" Myocardium?

The presence of surviving cardiac myocytes within post-MI regions has been repeatedly documented in humans[31,32] as well as in laboratory animals,[25–30,33] particularly in rats.[11,14,15,18,22–24,34–37] Moreover, the majority of these reports have shown that viable cardiac myocytes were predominantly seen in two distinct regions of the transmural scars, specifically, in the subendocardium and subepicardium of the LV wall. Therefore, the fact that viable cardiac myocytes remaining in these two regions of the scar had undergone noticeably opposite changes in transverse dimensions during the course of 12 post-MI weeks is a fundamental finding of this study. Taking into consideration our current, as well as previous findings,[14] we believe that progressive atrophy of subendocardial myocytes could be a result of excessive deposition of fibroelastic tissue around individual cells that may interfere with their access to nutrients and oxygen and, thus, lead to progressive cell starvation. However, the apparent enlargement of subepicardial myocytes may, to an extent, be due to cell dedifferentiation similar to that described in cardiac myocytes surviving in the MI border zone.[38,39] It is important to emphasize that because nearly the same array of heterogeneous structural alterations has been previously reported among viable cardiac myocytes from "hibernating" myocardium,[40–42] it seems reasonable to suggest that adult cardiac myocytes surviving in the transmural scar resemble those seen in chronically ischemic but viable myocardium.

Furthermore, although we did not examine the functional capability of surviving cardiac myocytes, the continual protein expression of contractile and muscle-specific intermediate filaments, as well as the presence of organized sarcomeres, serve as a confirmation that even in "functional isolation," viable myocytes of the scar can maintain their contractile apparatus for an extended period of time. In addition, the persistent expression of connexin 43 protein and its accumulation between adjacent cells in a pattern resembling gap junctions suggests that surviving cardiac myocytes within the scars continue to preserve intercellular ionic coupling, typical of a functional syncytium. Taken together, these findings support the idea that the spared groups of cardiac myocytes surviving in transmural post-MI scars might be capable of recovering from their dormant state after the reestablishment of adequate arterial blood perfusion, analogous to chronically ischemic, "hibernating" myocardium.[41]

Can the Residual Coronary Venous System in Transmural Post-MI Scar Provide a Route for Nutritive Blood Supply to Viable Cardiac Myocytes?

It is important to emphasize that, according to our results, the fractional volume of surviving cardiac myocytes remained relatively comparable in scars between 4 and 12 post-MI weeks, suggesting that the regional microenvironment in certain areas of the mature scar was able to facilitate the extended survival of adult cardiac myocytes. Taking into consideration the fact that in our rat model of a chronic MI, as well as in similar studies done by others,[11,15,22–24] the left coronary artery remained permanently occluded for the duration of the experimental period, the presence of surviving cardiac myocytes, especially in remote areas of the large transmural scar, remains not fully understood. These observations are even more puzzling recognizing the fact that adult rats do not have patent collateral vessels between left and right coronary arteries.[19–21] In this regard, it is important to stress that mature post-MI scars were shown

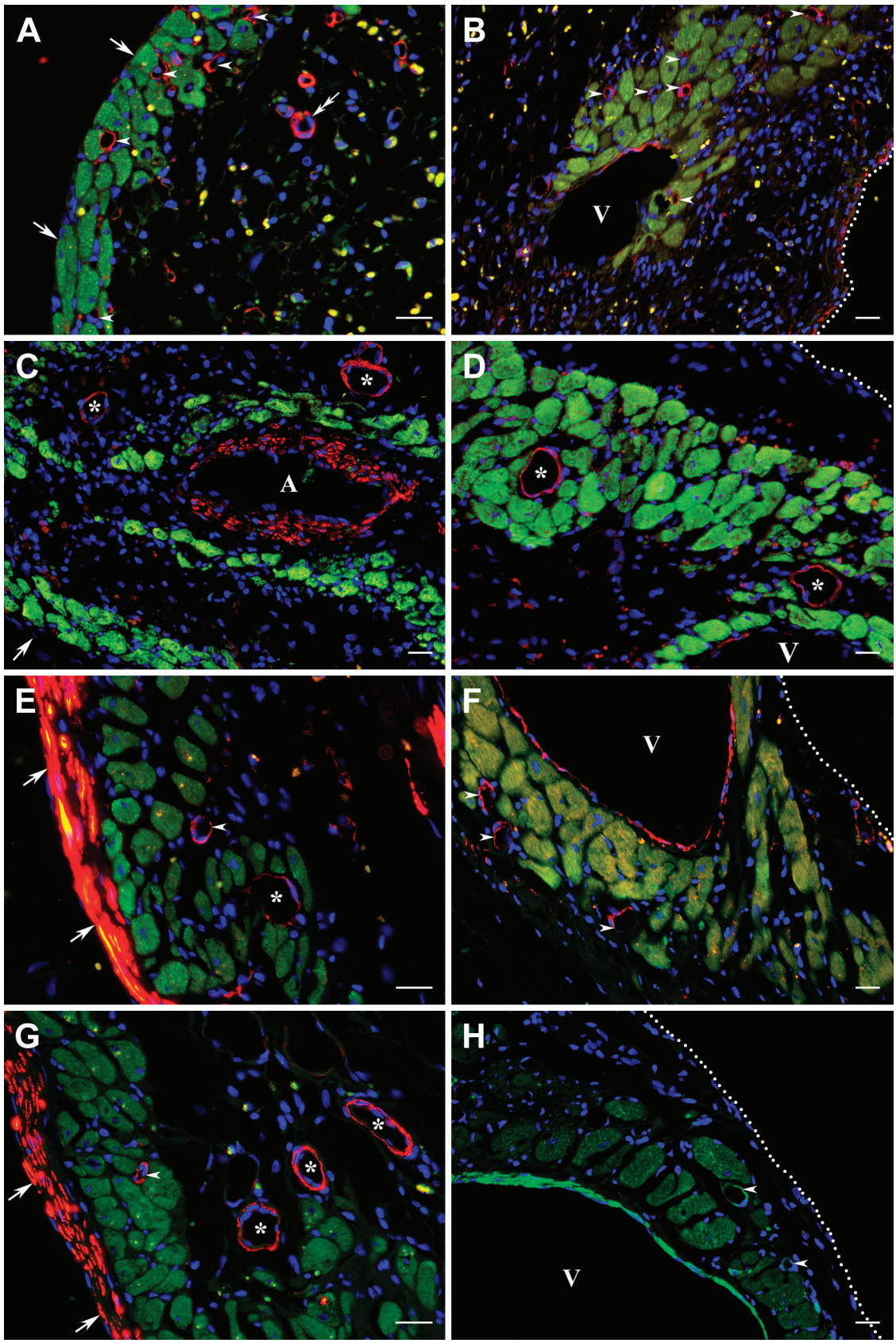

(continued)

Figure 8. Immunofluorescence micrographs demonstrating the presence of resistance microvessels accompanying the viable cardiac myocytes in 1-week-old (A, B), 2-week-old (C, D), 4-week-old (E, F), and 8-week-old (G, H) transmural post-MI scars. The cardiac myocytes surviving within subendocardial (A, C, E, G) and subepicardial (B, D, F, H) regions of the corresponding scars are visualized using immunostaining with an antibody against cardiac MHC β-isoform (green color), whereas the resistance microvessels are identified with an antibody against α-SM actin (red color in A–G and bright green color in H). Note that in addition to small resistance microvessels (arrowheads and asterisks), the α-SM actin-positive immunostaining is present in the walls of a former coronary artery (A in micrograph C) and large subepicardial veins (V) as well as within the layer of subendocardial myofibroblasts in E and G. In all micrographs, nuclei are counterstained with DAPI (blue color). Furthermore, in A, C, E, and G, arrows point to the endocardium, whereas in B, D, F, and H, the white dotted lines mark the epicardial border. It is important to highlight that although the existence of α-SM actin expression in these microvessels suggests their belonging to resistance vasculature, primarily to small- and medium-sized arterioles, phenotypically, most of them resemble the arterialized thin-walled venous vessels, such as postcapillary venules (arrowheads) and small veins (asterisks). The latter assumption is also corroborated by the fact that according to the pattern of α-SM actin-positive immunoreactivity, such "resistance-like" microvessels often display a discontinuous and relatively thin muscular wall in comparison with their luminal diameter. For comparison, the double arrow in micrograph A points to a relatively typical arteriolar vessel seen inside the developing granulation tissue. Scale bars are 20 μm (A–H). Abbreviations: MI, myocardial infarction; MHC, myosin heavy chain; SM, smooth muscle; DAPI, 4′,6-diamidino-2-phenylindole.

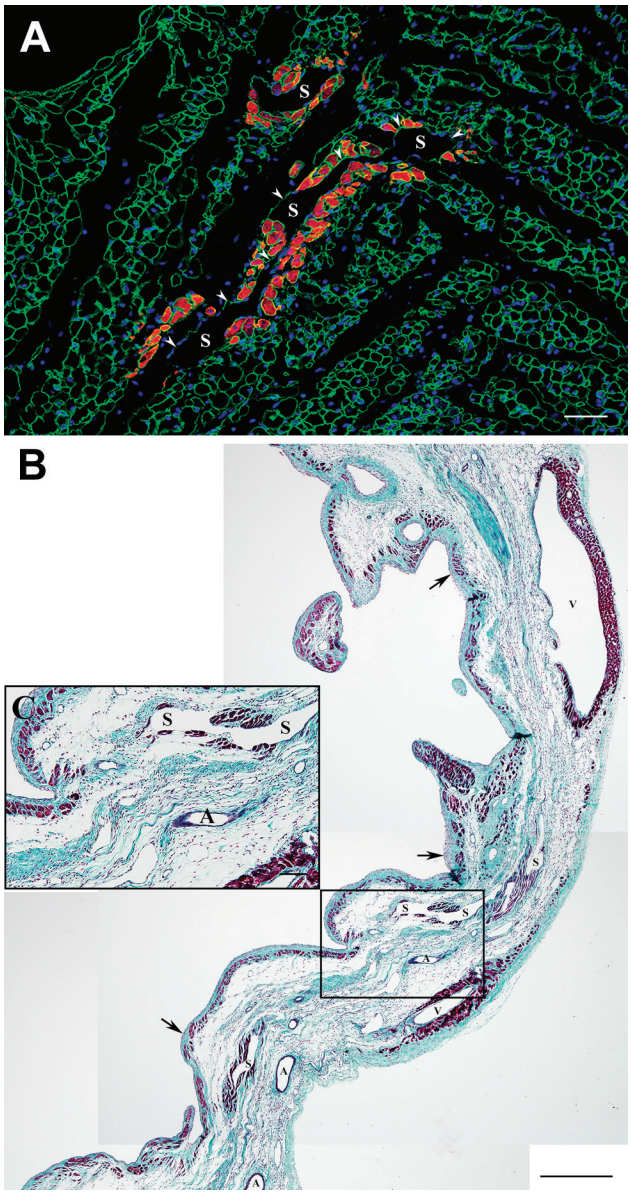

(continued)

Figure 9. Immunofluorescence and Masson's trichrome stained micrographs displaying the viable cardiac myocytes in the vicinity of intramural sinusoidal vessels within 1-week-old (A) and 4-week-old (B, C) transmural post-MI scars. (A) High-power view of an immunofluorescence micrograph from the intramural region of a 1-week-old scar showing the viable cardiac actin-positive myocytes (red color) around the thin-walled sinusoidal vessels (S), which are outlined with the laminin-positive basement membranes (green color). Nuclei are counterstained with DAPI (blue color). Note that one of two depicted sinusoidal vessel (arrowheads) extends for a relatively long distance within the scar. (B) Low-power view of a representative transversal section through a 4-week-old scar stained with Masson's trichrome stain demonstrating the typical sites of cardiac myocytes survival (dark red color), including the areas beneath the endocardium (arrows) and epicardium, particularly around the large subepicardial veins (V), and, most importantly, along the intramural venous sinusoids (S). Notice a complete absence of viable cardiac myocytes around the arterial vessels (A). (C) High-power view of the area outlined by a black box in B showing the presence of viable cardiac myocytes intramurally, along the thin-walled sinusoidal vessels (S). It is important to emphasize that long-term survival of mature cardiac myocytes around such vascular structures suggests their functional potency for persistent blood perfusion. Scale bars are 50 μm (A), 500 μm (B), and 100 μm (C). Abbreviations: MI, myocardial infarction; DAPI, 4′,6-diamidino-2-phenylindole.

to have a large number of patent venous vessels, particularly in subepicardial and subendocardial regions of the scar,[36] which were often seen surrounded by viable cardiac myocytes.[14,15,22,35,36,43,44] Our current observations have further substantiated these findings by demonstrating that the residual veins surrounded by viable cardiac myocytes could persist in the scar for weeks following permanent ligation of the coronary artery. The latter suggests that the nutritive and oxygen content of the blood present inside these venous vessels could be sufficient to support the long-term viability of adjacent cardiac myocytes. However, the question concerning the origin and direction of the blood flow in such

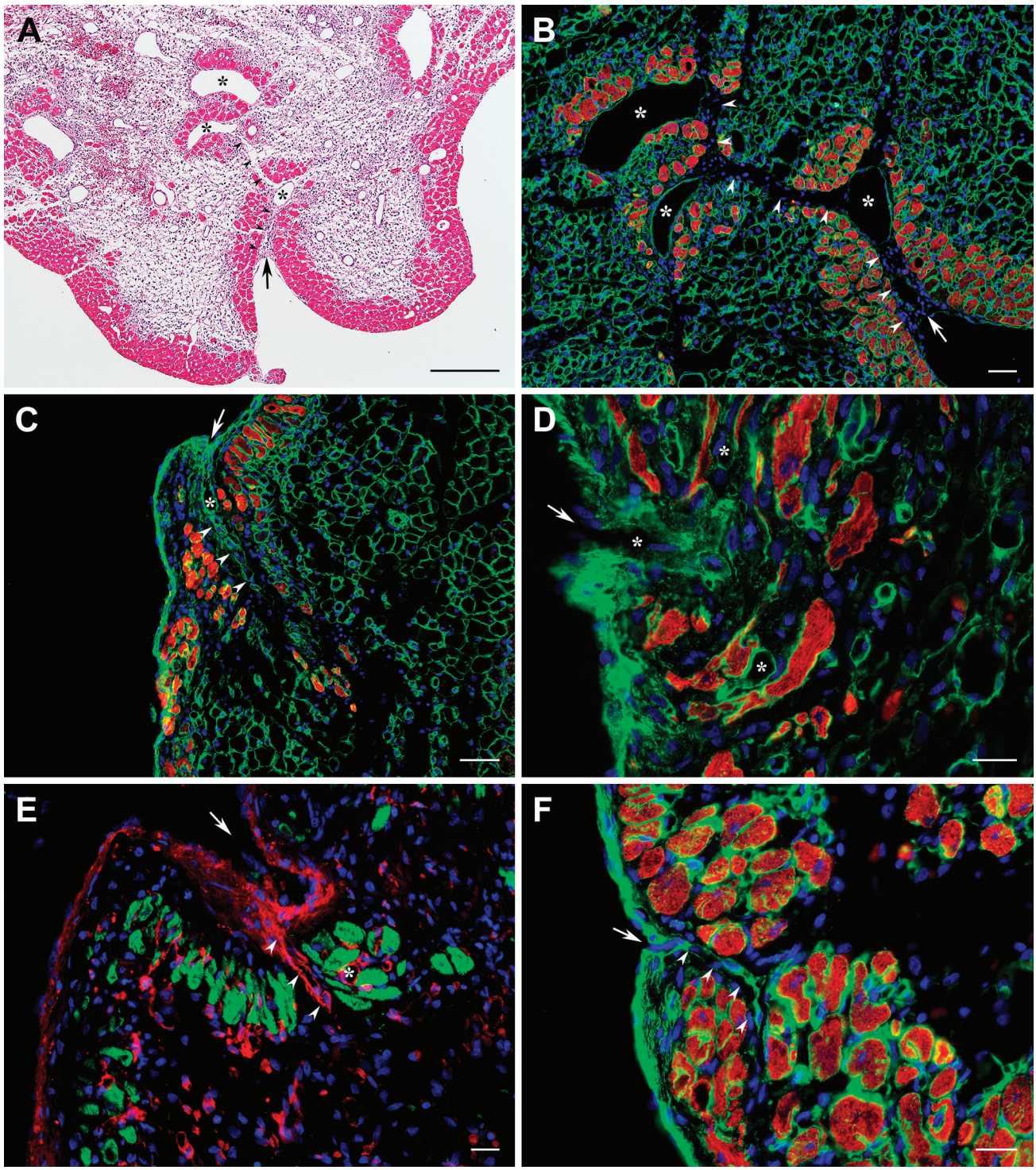

Figure 10. High-power micrographs demonstrating the existence of the vascular orifices (arrows), probably from Thebesian veins or venous channels, on the endocardial surface of 3-day-old (A, B), 1-week-old (C, D), and 2-week-old (E, F) transmural post-MI scars that connect the subendocardial vascular network associated with surviving cardiac myocytes to the LV cavity. The representative micrographs are stained either with hematoxylin and eosin (A) or immunofluorescence (B–F). In all micrographs, asterisks denote the profiles of the vascular structures, including venous microvessels and sinusoids, whereas arrowheads expose the vascular channels linking endocardial orifices to subendocardial vessels. In immunofluorescence micrographs B, C, D, and F, the viable cardiac myocytes (red color) are visualized using double immunostaining with antibodies against either cardiac actin (B, D, and F) or cardiac MHC β-isoform (C) and

(continued)

Figure 10. (continued)

laminin (green color). In immunofluorescence micrograph E, the viable cardiac myocytes (green color) are visualized using immunostaining with an anticardiac MHC β-isoform antibody, whereas vascular structures (red color) are revealed with the GS-IB_4 lectin staining. In all immunofluorescence micrographs, nuclei are counterstained with DAPI (blue color). Note, in micrographs A, B, and C, besides the subendocardial region, the surviving cardiac myocytes are also seen intramurally, extending deeper along the venous vascular structures, most likely Thebesian veins and venous sinusoids, which are directly linked to LV cavity. Scale bars are 200 μm (A), 50 μm (C), and 20 μm (B, D, E, and F). Abbreviations: MI, myocardial infarction; MHC, myosin heavy chain; LV, left ventricular; GS-IB_4, Griffonia Simplicifolia isolectin IB_4; DAPI, 4′,6-diamidino-2-phenylindole.

vascular structures, particularly those associated with viable cardiac myocytes, remains debatable.

For almost a century, it has been known that the architecture of the coronary venous system is more complex than that of the arterial bed.[45,46] In the left ventricle, along with conventional cardiac veins, this system includes intramyocardial sinusoids, subendocardial and subepicardial venous plexuses as well as Thebesian veins (valveless venous channels), which directly connect the coronary venous system to the LV cavity.[47,48] Considering the fact that the residual vessels in mature scars continued to be perfused with blood several weeks after permanent ligation of the left coronary artery,[18,22,34,43] it seems reasonable to assume that Thebesian veins might serve as a potential route for arterial blood inflow into the coronary veins of the LV wall, particularly following ligation of the left coronary artery. However, until now, the origin of arterial blood inflow into the vessels remained poorly specified. Taking into consideration the fact that we found patent orifices of Thebesian veins on the endocardial surface of the transmural scars, which appeared analogous to those reported previously by others,[49] we have hypothesized that the venous vessels of the scar might be supplied with the arterial blood through these channels. Moreover, our finding that microspheres injected into the LV cavity of post-MI rats could be found inside the lumen of venular-type vessels in the scars further supports this idea. In addition, the presence of surviving cardiac myocytes around thin-walled venous sinusoids within the intramural region of the infarcted LV wall might indicate the existence of patent vascular routes throughout the thickness of the scar.

Is Preservation of the Functional Microvascular Bed Imperative for Persistent Survival of Cardiac Myocytes in Transmural Post-MI Scar?

One of the important observations that was made in our current study has proven the earlier findings reported by us[14] and others[18,29,34,43] that the viable cardiac myocytes in transmural scars continued to be supported by a well-organized network of perfused capillaries, even when positioned in close proximity to the LV cavity or large "nourishing" veins. These data clearly indicate that blood circulating through a local microcirculatory bed, rather than simple diffusion from LV lumen and veins, has been primarily responsible for the continual delivery of the nutrients and oxygen to the residual cardiac myocytes in post-MI scars.

Although it has become common knowledge that after MI, new microvessels form in the infarcted region to assist in resorption of necrotic myocytes and to nourish the developing granulation tissue,[15,25,26] it remains highly uncertain as to their potential involvement in the survival of remaining cardiac myocytes. In our current study, we also found that the highly vascularized granulation tissue became distributed throughout the scar by the end of first post-MI week. However, a few weeks later, the majority of newly formed capillaries had disappeared from the maturing fibrous tissue in the sequence that was previously reported.[15,25] This finding suggests that the neovasculature associated with granulation tissue could not provide a sustainable route for delivery of nutrients and oxygen to viable cardiac myocytes in the scars. In this regard, it is important to emphasize that the microvessels seen in the vicinity of viable cardiac myocytes between 3 days and 12 weeks post-MI remained unaffected by the process of scar maturation. This finding evidently supports the idea that these two microcirculatory beds have different anatomical origins as well as a source of blood perfusion.

The above hypothesis can be further corroborated by the fact that almost all arteriolar-like (α-SM actin-positive) vessels seen in microcirculatory beds associated with the viable cardiac myocytes did not appear to be typical small diameter, thick-walled arterioles, but rather resembled the large diameter, thin-walled venules that have undergone a remodeling process called arteriolization. Taking into account that such process, that is, the acquisition of the arteriolar-like phenotype by the venular-type vessels, can primarily be caused by the increased hemodynamic load on the vessel wall,[50] it is reasonable to propose that ligation of the coronary artery might redistribute the blood pressure gradient inside the remaining coronary vascular

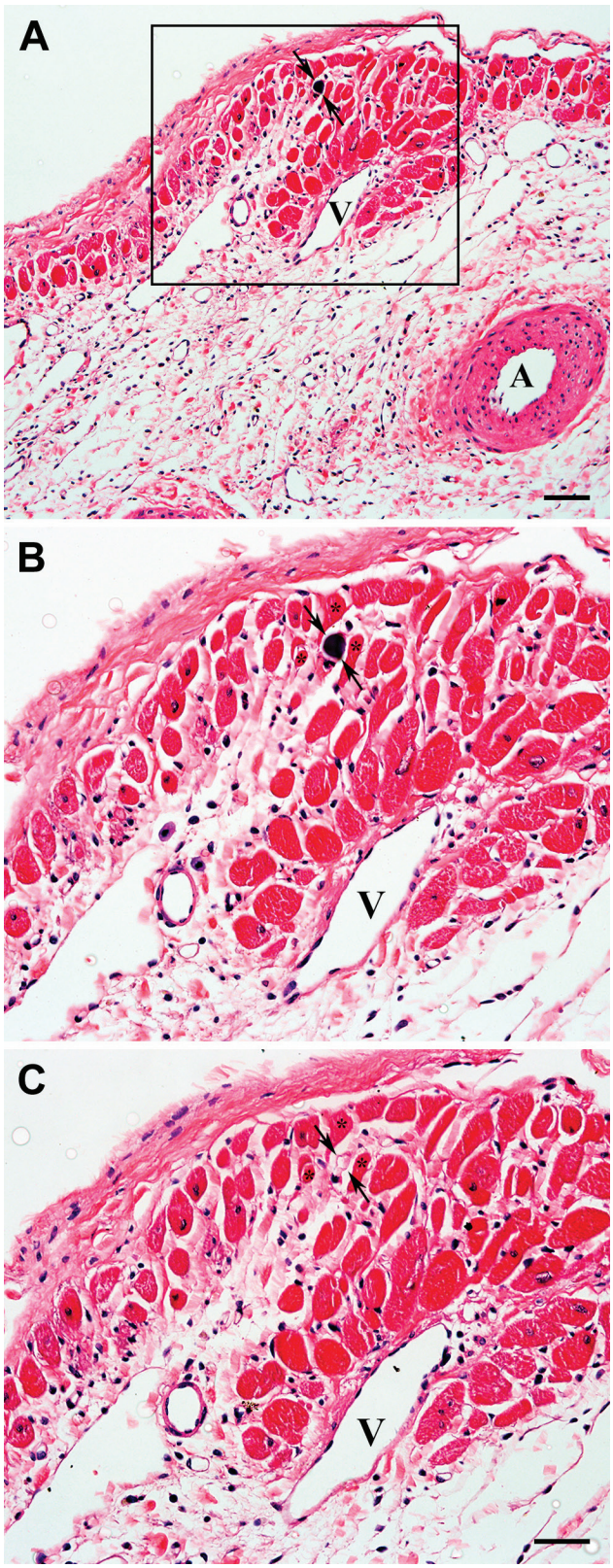

Figure 11. Hematoxylin and eosin–stained micrographs demonstrating the presence of a microsphere within a venular-like *(continued)*

Figure 11. (continued)

microvessel associated with the group of viable cardiac myocytes in representative 8-week-old transmural post-MI scar. (A) Low-power view of the subepicardial region revealing a microsphere (arrows) surrounded by surviving cardiac myocyte. (B) High-power view of an area outlined by a black box in A displaying the same microsphere (arrows) in a microvessel surrounded by three viable cardiac myocytes (asterisks). (C) High-power view of the same region shown in B (obtained from an adjacent serial section) demonstrating a profile of the microvessel in which a microsphere (arrows) has been detected. In all micrographs, arrows point to the location of a microsphere, whereas in B and C, the asterisks indicate the same cardiac myocytes located in the vicinity of the microsphere-containing microvessel. It is important to emphasize that the microsphere-containing microvessel has an apparent phenotypic resemblance of a venule. A and V indicate an artery and a vein, respectively. Scale bars are 50 μm (A) and 30 μm (B, C). Abbreviation: MI, myocardial infarction.

system in a way that permits significant retrograde inflow of arterial blood from the LV cavity into subendocardial and subepicardial microcirculatory beds through patent Thebesian vessels. In this regard, our current hypothesis is in accord with a model previously proposed by others[26,28,48] who consider sustainable retroperfusion of preexisting microvessels in subendocardial and subepicardial regions with oxygenated and nutrient-rich arterial blood from LV lumen as an essential mechanism preserving the small population of adult (mature) cardiac myocytes during acute and chronic phases of a large transmural MI caused by a permanent obstruction of the left coronary artery.

Study Limitations

This study has several major limitations. First, taking into account that long-term survival of cardiac myocytes in the scar could be caused by their functional and metabolic adaptations to the markedly diminished nutritive supply, it would be important to examine a dynamic pattern of their metabolism. Second, considering the fact that the level of oxygen was not directly assessed in the venous vessels of the scar, it has remained undetermined whether the residual venous network in the scar had a higher content of oxygenated blood compared with the veins in non-infarcted myocardium. Third, we did not perform angiographic or cast-based evaluation of the entire coronary arterial tree in the infarcted hearts to confirm it lacks anastomoses between coronary arteries and microvascular beds supplying the viable cardiac myocytes in the scars. Fourth, it would be of a great value to test the coupling of subepicardial veins to subendocardial plexuses via Thebesian vessels by retrograde infusion of the microspheres into the cardiac sinus or the great

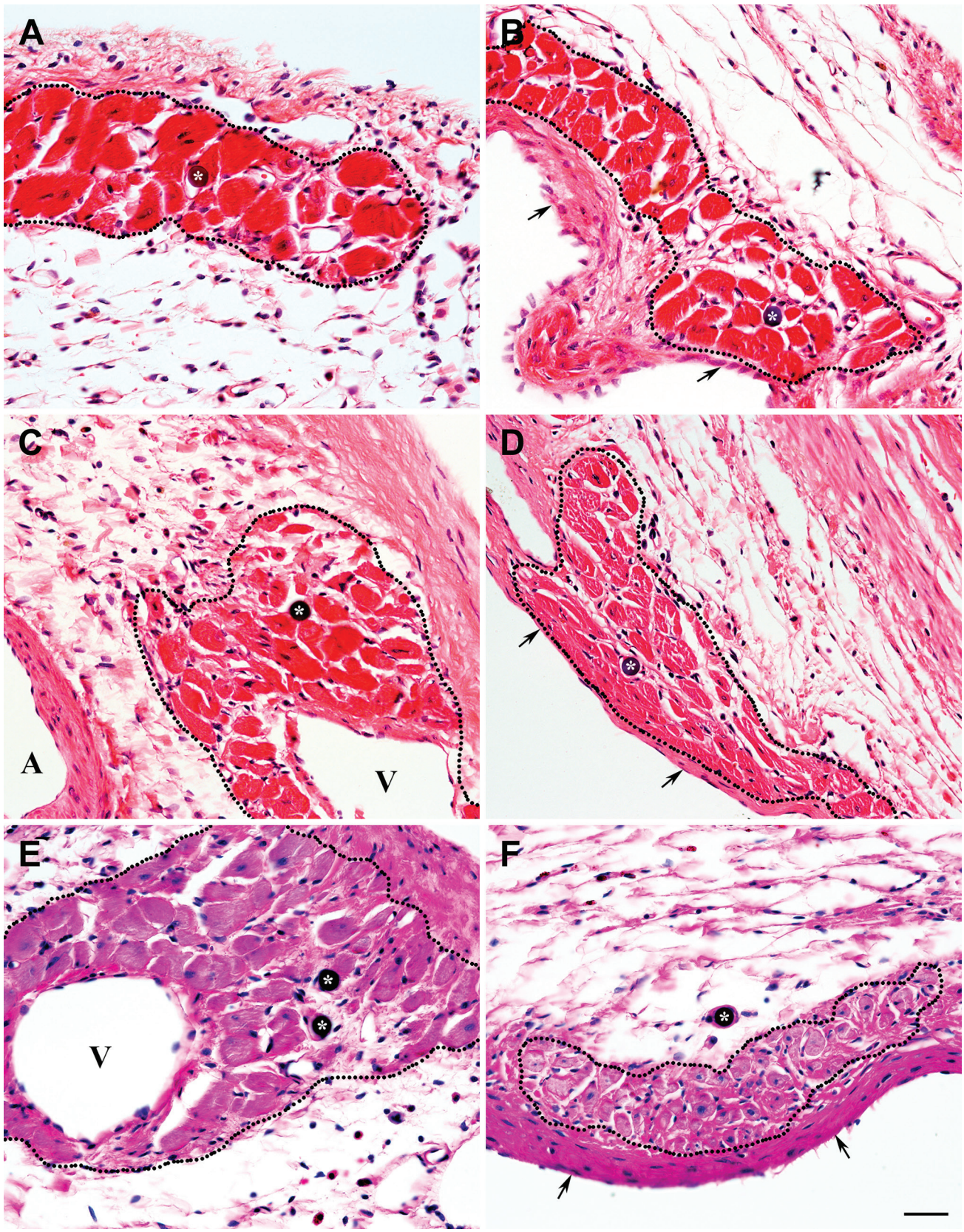

(continued)

Figure 12. Hematoxylin and eosin–stained micrographs demonstrating the presence of microspheres (asterisks) in the lumen of functional microvessels accompanying the viable cardiac myocytes in 4-week-old (A, B), 8-week-old (C, D), and 12-week-old (E, F) transmural post-MI scars. The clusters of cardiac myocytes surviving in subepicardial (A, C, E) and subendocardial (B, D, F) regions of the corresponding scars are outlined by the black dotted lines. In micrographs B, D, and F, arrows point to the endocardium, whereas in micrographs C and E, veins are indicated by V and an artery by A. It is important to emphasize that the presence of microspheres in microcirculatory beds associated with the viable cardiac myocyte suggest their functional potency. Moreover, structural appearance of a majority of thin-walled microsphere-containing microvessels points at their venous origin. Scale bar is 30 μm (A–F). Abbreviation: MI, myocardial infarction.

cardiac vein. Finally, the absence of a comprehensive ultrastructural evaluation of the arteriolar-like vessels accompanying the viable cardiac myocytes that have been seen containing microspheres does not allow for definitive validation of their true nature. Nevertheless, we believe that the findings provided in our current investigation are an important addition to the wealth of knowledge that may one day lead to the development of an optimal strategy to restore the functional myocardium in the place of fibrous post-MI scar.

Taken together, our data demonstrate that the long-term survival of mature cardiac myocytes in transmural post-MI scars of middle-aged rats relied on the preservation of local, functionally patent microcirculatory beds. These microcirculatory beds remained cohesive with the remnants of the preexisting venous system, which probably operated as a trans-scar conduit for oxygenated blood exchange between LV cavity and subepicardial veins. Furthermore, we believe that the regions of the scar showing the presence of surviving cardiac myocytes accompanied by patent microvascular networks can be a primary target for scar-modifying therapies, especially those geared toward using an endogenous source of contractile cells to restore functional myocardium in infarcted areas.

Acknowledgment

The authors thank Alice O'Connor for help with histological techniques.

Competing Interests

The author(s) declared no potential conflicts of interest with respect to the research, authorship, and/or publication of this article.

Author Contributions

All authors have contributed to this article as follows: planning (EID), acquisition of samples (EID), execution of experiments (CN, YB, EID), analysis of data (CN, YB, EID), writing of manuscript (CN, EID), and all authors have read and approved the manuscript as submitted.

Funding

The author(s) received no financial support for the research, authorship, and/or publication of this article.

Literature Cited

1. Frangogiannis NG. The mechanistic basis of infarct healing. Antioxid Redox Signal. 2006;8(11–12):1907–39. doi:10.1089/ars.2006.8.1907.
2. Richardson WJ, Clarke SA, Quinn TA, Holmes JW. Physiological implications of myocardial scar structure. Compr Physiol. 2015;5(4):1877–909. doi:10.1002/cphy.c140067.
3. Gajarsa JJ, Kloner RA. Left ventricular remodeling in the post-infarction heart: a review of cellular, molecular mechanisms, and therapeutic modalities. Heart Fail Rev. 2011;16(1):13–21. doi:10.1007/s10741-010-9181-7.
4. Gaballa MA, Goldman S. Ventricular remodeling in heart failure. J Card Fail. 2002;8(6 Suppl):S476–85. doi:10.1054/jcaf.2002.129270.
5. Pfeffer MA, Braunwald E. Ventricular remodeling after myocardial infarction. Experimental observations and clinical implications. Circulation. 1990;81(4):1161–72.
6. Rog-Zielinska EA, Norris RA, Kohl P, Markwald R. The living scar—cardiac fibroblasts and the injured heart. Trends Mol Med. 2016;22(2):99–114. doi:10.1016/j.molmed.2015.12.006.
7. Khanabdali R, Rosdah AA, Dusting GJ, Lim SY. Harnessing the secretome of cardiac stem cells as therapy for ischemic heart disease. Biochem Pharmacol. 2016;113:1–11. doi:10.1016/j.bcp.2016.02.012.
8. Holmes JW, Laksman Z, Gepstein L. Making better scar: emerging approaches for modifying mechanical and electrical properties following infarction and ablation. Prog Biophys Mol Biol. 2016;120(1–3):134–48. doi:10.1016/j.pbiomolbio.2015.11.002.
9. du Pre BC, Doevendans PA, van Laake LW. Stem cells for cardiac repair: an introduction. J Geriatr Cardiol. 2013;10(2):186–97. doi:10.3969/j.issn.1671-5411.2013.02.003.
10. Zornoff LA, Paiva SA, Minicucci MF, Spadaro J. Experimental myocardium infarction in rats: analysis of the model. Arq Bras Cardiol. 2009;93(4):434–40, 26–32.
11. Hochman JS, Bulkley BH. Expansion of acute myocardial infarction: an experimental study. Circulation. 1982;65(7):1446–50.
12. Johns TN, Olson BJ. Experimental myocardial infarction. I. A method of coronary occlusion in small animals. Ann Surg. 1954;140(5):675–82.
13. Dedkov EI, Bogatyryov Y, Pavliak K, Santos AT, Chen YF, Zhang Y, Pingitore A. Sex-related differences in intrinsic myocardial properties influence cardiac function in middle-aged rats during infarction-induced

left ventricular remodeling. Physiol Rep. 2016;4(11). doi:10.14814/phy2.12822.
14. Bogatyryov Y, Tomanek RJ, Dedkov EI. Structural composition of myocardial infarction scar in middle-aged male and female rats: does sex matter? J Histochem Cytochem. 2013;61(11):833–48. doi:10.1369/0022155413499794.
15. Fishbein MC, Maclean D, Maroko PR. Experimental myocardial infarction in the rat: qualitative and quantitative changes during pathologic evolution. Am J Pathol. 1978;90(1):57–70.
16. Sun Y, Kiani MF, Postlethwaite AE, Weber KT. Infarct scar as living tissue. Basic Res Cardiol. 2002;97(5):343–7. doi:10.1007/s00395-002-0365-8.
17. Muller-Ehmsen J, Peterson KL, Kedes L, Whittaker P, Dow JS, Long TI, Laird PW, Kloner RA. Rebuilding a damaged heart: long-term survival of transplanted neonatal rat cardiomyocytes after myocardial infarction and effect on cardiac function. Circulation. 2002;105(14):1720–6.
18. Dai W, Hale SL, Martin BJ, Kuang JQ, Dow JS, Wold LE, Kloner RA. Allogeneic mesenchymal stem cell transplantation in postinfarcted rat myocardium: short- and long-term effects. Circulation. 2005;112(2):214–23. doi:10.1161/CIRCULATIONAHA.104.527937.
19. Spadaro J, Fishbein MC, Hare C, Pfeffer MA, Maroko PR. Characterization of myocardial infarcts in the rat. Arch Pathol Lab Med. 1980;104(4):179–83.
20. Taira Y, Kanaide H, Nakamura M. The distribution of ischaemia in perfused Wistar rat hearts following coronary artery occlusion. Br J Exp Pathol. 1985;66(5):613–21.
21. Maxwell MP, Hearse DJ, Yellon DM. Species variation in the coronary collateral circulation during regional myocardial ischaemia: a critical determinant of the rate of evolution and extent of myocardial infarction. Cardiovasc Res. 1987;21(10):737–46.
22. Kalkman EA, van Haren P, Saxena PR, Schoemaker RG. Regionally different vascular response to vasoactive substances in the remodelled infarcted rat heart; aberrant vasculature in the infarct scar. J Mol Cell Cardiol. 1997;29(5):1487–97. doi:10.1006/jmcc.1997.0388.
23. Boyle MP, Weisman HF. Limitation of infarct expansion and ventricular remodeling by late reperfusion. Study of time course and mechanism in a rat model. Circulation. 1993;88(6):2872–83.
24. Rutherford SL, Trew ML, Sands GB, LeGrice IJ, Smaill BH. High-resolution 3-dimensional reconstruction of the infarct border zone: impact of structural remodeling on electrical activation. Circ Res. 2012;111(3):301–11. doi:10.1161/CIRCRESAHA.111.260943.
25. Virag JI, Murry CE. Myofibroblast and endothelial cell proliferation during murine myocardial infarct repair. Am J Pathol. 2003;163(6):2433–40. doi:10.1016/S0002-9440(10)63598-5.
26. Ring PA. Myocardial regeneration in experimental ischaemic lesions of the heart. J Pathol Bacteriol. 1950;62(1):21–7.
27. Factor SM, Sonnenblick EH, Kirk ES. The histologic border zone of acute myocardial infarction—islands or peninsulas? Am J Pathol. 1978;92(1):111–24.
28. Forman R, Cho S, Factor SM, Kirk ES. Acute myocardial infarct extension into a previously preserved subendocardial region at risk in dogs and patients. Circulation. 1983;67(1):117–24.
29. Kramer MF, Kinscherf R, Aidonidis I, Metz J. Occurrence of a terminal vascularisation after experimental myocardial infarction. Cell Tissue Res. 1998;291(1):97–105.
30. Bowen FW, Hattori T, Narula N, Salgo IS, Plappert T, Sutton MG, Edmunds LH Jr. Reappearance of myocytes in ovine infarcts produced by six hours of complete ischemia followed by reperfusion. Ann Thorac Surg. 2001;71(6):1845–55.
31. Fenoglio JJ Jr, Pham TD, Harken AH, Horowitz LN, Josephson ME, Wit AL. Recurrent sustained ventricular tachycardia: structure and ultrastructure of subendocardial regions in which tachycardia originates. Circulation. 1983;68(3):518–33.
32. de Bakker JM, Coronel R, Tasseron S, Wilde AA, Opthof T, Janse MJ, van Capelle FJ, Becker AE, Jambroes G. Ventricular tachycardia in the infarcted, Langendorff-perfused human heart: role of the arrangement of surviving cardiac fibers. J Am Coll Cardiol. 1990;15(7):1594–607.
33. Factor SM, Okun EM, Kirk ES. The histological lateral border of acute canine myocardial infarction. A function of microcirculation. Circ Res. 1981;48(5):640–49.
34. Dai W, Wold LE, Dow JS, Kloner RA. Thickening of the infarcted wall by collagen injection improves left ventricular function in rats: a novel approach to preserve cardiac function after myocardial infarction. J Am Coll Cardiol. 2005;46(4):714–9. doi:10.1016/j.jacc.2005.04.056.
35. Zhang RL, Christensen LP, Tomanek RJ. Chronic heart rate reduction facilitates cardiomyocyte survival after myocardial infarction. Anat Rec. 2010;293(5):839–48. doi:10.1002/ar.21081.
36. Nelissen-Vrancken HJ, Debets JJ, Snoeckx LH, Daemen MJ, Smits JF. Time-related normalization of maximal coronary flow in isolated perfused hearts of rats with myocardial infarction. Circulation. 1996;93(2):349–55.
37. Hochman JS, Choo H. Limitation of myocardial infarct expansion by reperfusion independent of myocardial salvage. Circulation. 1987;75(1):299–306.
38. Dedkov EI, Stadnikov AA, Russell MW, Borisov AB. Formation of leptofibrils is associated with remodelling of muscle cells and myofibrillogenesis in the border zone of myocardial infarction. Micron. 2007;38(6):659–67. doi:10.1016/j.micron.2006.08.006.
39. Driesen RB, Verheyen FK, Dijkstra P, Thone F, Cleutjens JP, Lenders MH, Ramaekers FC, Borgers M. Structural remodelling of cardiomyocytes in the border zone of infarcted rabbit heart. Mol Cell Biochem. 2007;302(1–2):225–32. doi:10.1007/s11010-007-9445-2.
40. Heusch G, Schulz R, Rahimtoola SH. Myocardial hibernation: a delicate balance. Am J Physiol Heart Circ Physiol. 2005;288(3):H984–99. doi:10.1152/ajpheart.01109.2004.
41. Slezak J, Tribulova N, Okruhlicova L, Dhingra R, Bajaj A, Freed D, Singal P. Hibernating myocardium:

pathophysiology, diagnosis, and treatment. Can J Physiol Pharmacol. 2009;87(4):252–65. doi:10.1139/Y09-011.
42. Depre C, Vatner SF. Cardioprotection in stunned and hibernating myocardium. Heart Fail Rev. 2007;12(3–4):307–17. doi:10.1007/s10741-007-9040-3.
43. Wang B, Ansari R, Sun Y, Postlethwaite AE, Weber KT, Kiani MF. The scar neovasculature after myocardial infarction in rats. Am J Physiol Heart Circ Physiol. 2005;289(1):H108–13. doi:10.1152/ajpheart.00001.2005.
44. Dusek J, Rona G, Kahn DS. Healing process in the marginal zone of an experimental myocardial infarct. Findings in the surviving cardiac muscle cells. Am J Pathol. 1971;62(3):321–38.
45. Kassab GS, Navia JA, March K, Choy JS. Coronary venous retroperfusion: an old concept, a new approach. J Appl Physiol (1985). 2008;104(5):1266–72. doi:10.1152/japplphysiol.00063.2008.
46. Echeverri D, Cabrales J, Jimenez A. Myocardial venous drainage: from anatomy to clinical use. J Invasive Cardiol. 2013;25(2):98–105.
47. Tsang JC, Chiu RC. The phantom of "myocardial sinusoids": a historical reappraisal. Ann Thorac Surg. 1995;60(6):1831–5. doi:10.1016/0003-4975(95)00721-0.
48. Ansari A. Anatomy and clinical significance of ventricular Thebesian veins. Clin Anat. 2001;14(2):102–10. doi:10.1002/1098-2353(200103)14:2<102::AID-CA1018>3.0.CO;2-4.
49. Rosinia FA, Low FN.Scanning electron microscopy of Thebesian ostia (microdissection by ultrasonication: enzymatic digestion). Scan Electron Microsc. 1986(Pt 4):1363–9.
50. Van Gieson EJ, Murfee WL, Skalak TC, Price RJ. Enhanced smooth muscle cell coverage of microvessels exposed to increased hemodynamic stresses in vivo. Circ Res. 2003;92(8):929–36.